LBL-15488
Preprint c.2

Lawrence Berkeley Laboratory

UNIVERSITY OF CALIFORNIA

RECEIVED
LAWRENCE
BERKELEY LABORATORY

FEB 18 1983

LIBRARY AND
DOCUMENTS SECTION

Materials & Molecular Research Division

Submitted to the Journal of Applied Physics

SUBSTITUTIONAL PLACEMENT OF PHOSPHORUS IN ION IMPLANTED SILICON BY RECRYSTALLIZING AMORPHOUS/ CRYSTALLINE INTERFACE

D.K. Sadana, J. Washburn, and C.W. Magee

September 1982

TWO-WEEK LOAN COPY

This is a Library Circulating Copy which may be borrowed for two weeks. For a personal retention copy, call Tech. Info. Division, Ext. 6782.

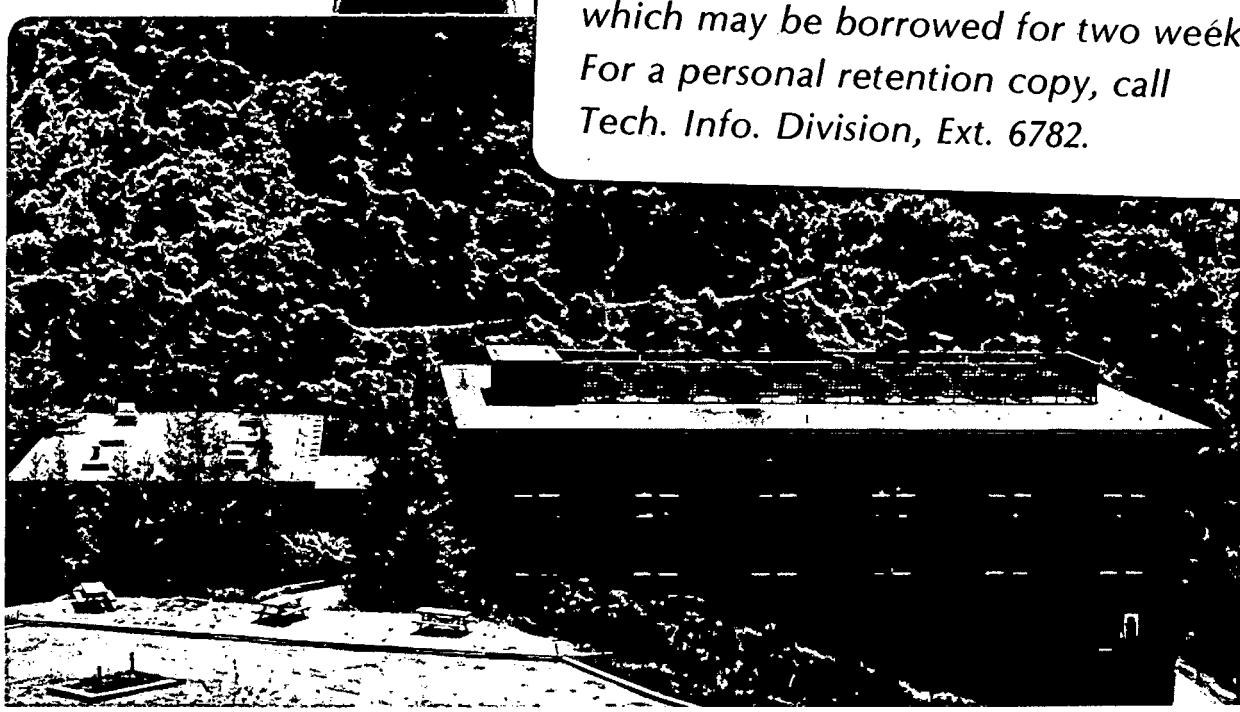

Prepared for the U.S. Department of Energy under Contract DE-AC03-76SF00098

LBL-15488 c.2

DISCLAIMER

This document was prepared as an account of work sponsored by the United States Government. While this document is believed to contain correct information, neither the United States Government nor any agency thereof, nor the Regents of the University of California, nor any of their employees, makes any warranty, express or implied, or assumes any legal responsibility for the accuracy, completeness, or usefulness of any information, apparatus, product, or process disclosed, or represents that its use would not infringe privately owned rights. Reference herein to any specific commercial product, process, or service by its trade name, trademark, manufacturer, or otherwise, does not necessarily constitute or imply its endorsement, recommendation, or favoring by the United States Government or any agency thereof, or the Regents of the University of California. The views and opinions of authors expressed herein do not necessarily state or reflect those of the United States Government or any agency thereof or the Regents of the University of California.

SUBSTITUTIONAL PLACEMENT OF PHOSPHORUS IN ION IMPLANTED SILICON BY RECRYSTALLIZING AMORPHOUS/CRYSTALLINE INTERFACE

D. K. Sadana and J. Washburn
Lawrence Berkeley Laboratory and
Department of Materials Science and Mineral Engineering
University of California
Berkeley, CA 94720

and

C. W. Magee
David Sarnoff Research Center
RCA Laboratories
Princeton, NJ 08540

ABSTRACT

Ion implantation of P into (111) Si has been investigated by cross-sectional transmission electron microscopy (XTEM) and secondary ion mass spectrometry (SIMS). In the dose range $1x10^{15}$-$2x10^{16}$ cm^{-2} at 120 keV the formation and width of the amorphous (a) layers were sensitively dependent on wafer-temperature. The effect of dynamic annealing on the crystalline (c) to amorphous transformation, and the effect of amorphicity and roughness of the a/c interface on the formation of microtwins have been studied. It has been observed that the P atoms in the amorphous (a) region do not redistribute on subsequent annealing while the P atoms below the a/crystalline (c) interface diffuse rapidly into the Si substrate. The carrier concentration profiles from the annealed samples were found to follow the atomic profiles almost exactly over the depth range extending from the

surface to where the original a/c interface existed. However, in the deeper regions, the electrical activity was found to be dependent on the annealing temperature used. The different behavior of atomic and carrier concentration redistributions in the amorphous and crystalline regions has been explained by a model that assumes incorporation of impurity atoms on substitutional sites by the moving a/c interface on recrystallization. The P atoms in the deeper regions are believed to redistribute via an interstitial diffusion mechanism at low temperatures ($\leq 750^{\circ}C$) and eventually occupy substitutional sites at higher temperatures ($>800^{\circ}C$).

INTRODUCTION

Ion implantation of B, P and As is carried out routinely in laboratories around the world to fabricate junction devices. It has been reported that both B and P show deep tails in as-implanted Si.[1-5] The work of Hofker[2] and Blood[3] clearly established that the main mechanism of extended tail formation is channeling of a small fraction (2-3 percent) of these ions during random implantation. Since there is no suitable substitute for B as a p-type dopant in Si, B implantation is still carried out, but into already amorphitized Si substrates to minimize the channeling effects. A similar technique can be applied in the case of P to reduce the channeling effect, however, As is preferred over P because it does not show any anomalous effects during either the implantation or subsequent annealing.[6] Furthermore, the atomic radii of As and Si are nearly identical. Therefore, minimum lattice distortion takes place when As occupies substitutional site in the Si lattice.

From the electrical activation point of view, the P implants, especially at high doses ($\geq 10^{15} cm^{-2}$) give more electrical activity[7] as compared to As.[8-10] The formation of As dimers, trimers and other complexes is thought to be responsible for the reduced electrical activation. In this paper, recrystallization of completely and partly amorphous (a) regions in high dose P implanted (111)Si has been studied by transmission electron microscopy (TEM) and the distribution of structural defects has been directly compared with the P profile. The TEM studies show that microtwins nucleate when the

a/crystalline(c) interface advances towards the surface during subsequent annealing, but there is an incubation period before the nucleation occurs. Similar findings have been reported earlier for both Si and GaAs.[11,12] Remarkable differences are observed in P redistribution in the region that was originally amorphous from that which was originally non-amorphous [below the a/c interface]. Beam heating and its effect on the formation of the a layer and redistribution of P is also discussed. The lattice location (i.e., substitutional or interstitial) of the P atoms was determined from the electrical measurements. From these findings, it is possible to explain the effect of dynamic annealing on in situ recrystallization, the incubation period for the growth of microtwins in (111) Si and the anomalous redistribution and electrical behavior of P in Si.

EXPERIMENTAL

Phosphorous was implanted into B-doped (111) Si at either nominal room temperature or higher in the dose range 1×10^{15}-2×10^{16} cm^{-2} at 120 keV. These implantation conditions correspond to an 1ss theoretical projected range of 1500Å with a straggling of 530Å.[13] The implanted samples were subsequently annealed in the temperature range 750-950°C in a N_2 atmosphere.

The width of the amorphous/damaged layers in the as-implanted samples and the damage distribution in the annealed samples were obtained from cross-sectional TEM (XTEM) specimens.[14] Strong-beam bright-field and weak-beam dark-field methods were used on plan view specimens for defect analysis. The atomic profiles of phosphorus were

obtained by secondary ion mass spectrometry (SIMS) using a positive Cs ion source under ultra high vacuum conditions.[15] The carrier concentration versus depth profiles were obtained by the spreading resistance technique.

RESULTS

a. Unannealed Samples

The doses chosen in the present experiment were such that continuous amorphous layers extending to the surface should have been created. When the heating occurred during implantation, either the widths of the continuous amorphous layers were reduced (moderate heating case $\leq 100^{\circ}C$), or the amorphous layer could not form (severe heating case $\geq 300^{\circ}C$). For example, in the case of 10^{15} and $1.7 \times 10^{16} cm^{-2}$ implantations, the widths of the continuous amorphous layers were 2100Å and 2570Å, respectively (Figs. 1a and 3a). However, when a small amount of heating (100°C) was allowed to occur during the implantation, the width of the sample implanted with 10^{16} $P^{+}cm^{-2}$ instead of being ~2570Å, reduced to 1850Å (Fig. 2a) and a 650Å wide layer of small defect clusters appeared immediately below the a/c interface. The latter region would have been amorphous in the unheated samples. When the temperature rose to 300-400°C during 5×10^{15}-10^{16} $P^{+}cm^{-2}$ implantation, varying damage structures were created across the wafer and color bands appeared at the surface. A typical series of XTEM results from heated samples implanted at high doses is shown in Fig. 4. The sample chosen for this study corresponded to one of the regions which showed a color band at the surface.

The SIMS profiles of P from both room temperature and heated implantations are shown in Figs. 1c, 2c, 3b, and 5b. When no heating occurred during implantation, the profiles showed gaussian distributions with tails extending to depths of x4Rp. The depth of the tail increased marginally with increasing substrate temperature above RT. Figure 6 shows the P distributions in the tail regions (2Rp–4Rp) from various samples used in this study. The heating also resulted in a slight redistribution of P near the surface [0–(Rp+ΔRp)].

b. Annealed Samples

On subsequent heating of the $10^{15}cm^{-2}$ sample at 750°C, a high density of microtwins were formed in the region L extending from the surface to a depth of 1400Å followed by a layer M of dislocation loops and rods (not visible in the micrograph of Fig. 1b) at a mean depth of 2100Å from the surface. The latter region corresponds to the original a/c interface in this sample. Similar results have been obtained by earlier workers in (111) Si.[16–18] The individual layers were separated using a technique described elsewhere.[1] Comparison of the XTEM results from the unannealed and annealed samples shows that the a/c interface advanced by 700Å toward the surface before the microtwins were nucleated. In other words, there was an incubation period during the annealing before nucleation of the microtwins occurred.[11,12] The region which recrystallized during the incubation period was free of secondary defects. The incubation period seemed to increase with the implantation dose and was probably related to the amorphicity and roughness of the a/c interface. For example, in the $10^{16}cm^{-2}$

sample, where moderate heating (~100°C) occurred during implantation, it was not until the a/c interface advanced by ~1000Å toward the surface that the microtwins were nucleated (Fig. 2b). A band of dislocations was present below the original a/c interface at a mean depth of 2320Å from the surface and the entire implanted region contained a three dimensional dislocation network. The microtwins near the surface are marked in Fig. 2b. The samples that suffered severe heating during implantation and showed color bands at the surface, did not contain any twins after annealing at 837°C. Instead, a high density of fine defect clusters, a dislocation network and two bands of dislocation loops were present at different depths in this sample (Fig. 5a).

The atomic profiles of P from the annealed samples showed interesting behavior. In general, the surface region showed no redistribution of P for either unheated or heated (during implantation) samples and the P atoms appeared to be pinned on subsequent annealing at ~850°C while the deeper parts showed pronounced diffusion effects. The width of the pinned P region was dependent on the dose. For example, the $10^{15}cm^{-2}$ (unheated) sample annealed at 750°C showed pinning in the region 0-1400Å (Fig.1b) while the width of the pinned regions in the $5x10^{15}cm^{-2}$ (heated), $10^{16}cm^{-2}$ (moderately heated) and $1.7x10^{16}cm^{-2}$ (unheated) samples annealed at 837°C were 2200Å, 2800Å and 2600Å, respectively (Figs. 5b, 2b, and 3b). The P profiles beyond this depth showed rapid diffusion to depths >0.6μm. Comparison of the widths of the pinned region in Figs. 1c, 2c, 3c and 5c with those of

the a regions in the unannealed samples (Figs. 1a, 2a, 3a and 4) shows that the two match closely except for the $10^{15}cm^{-2}$ sample where the width of the a region (Fig. 1a) was greater than the width of the pinned P region (Fig. 1c). At higher annealing temperature (950°C), the difference in the redistribution behavior of P near the surface and deeper regions was no longer evident (Fig. 7b), and both regions showed normal diffusion effects.

DISCUSSION

a. Unannealed Samples: Formation of α Layer and Dynamic Annealing

For low dose rate (a few $\mu A\ cm^{-2}$) implantation of Si wafers with good thermal contact to the heat sink, an amorphous layer is expected to form first at $0.7Rp$[19] and then broaden as the dose increases. At a certain critical dose, the amorphous layer will extend all the way to the surface (Fig. 1a). However, prolonged implantation, especially of wafers with poor thermal contact, may cause heating of the order of 100°C even at low dose rates. In the case of high dose rate implantation, if the continuous a layer has already formed before appreciable heating of the wafer occurs, the a layer will begin to recrystallize at the only a/c interface available and the width of the a layer will reduce on further implantation. This is the case with the sample in Fig. 2. The continuous layer in this sample should have been ~2570Å wide as was the case with the sample of Fig. 3a. However, due to the poor thermal contact, wafer-heating occurred and in situ recrystallization reduced the width of the a layer to 1850Å (Fig. 2a). For high dose rate (several hundred μAcm^{-2}) implanted wafers with

poor thermal contacts, a continuous layer may never form during the implantation (Figs. 4b-4e). Under these conditions, either buried amorphous layers (Figs. 4b-4d) or a buried band of small dislocation loops without any amorphous material may result (Fig. 4e). When appreciable heating of the wafer begins to occur after only a buried amorphous layer has formed (Fig. 4b), in situ recrystallization takes place at both the upper and lower a/c interfaces.[20]

The implantation assisted regrowth of amorphous material will be referred to as dynamic annealing. Details of the effects of dynamic annealing on the crystalline to amorphous transformation are described elsewhere.[21,22] In brief, under dynamical annealing conditions, radiation damage may cause a net reduction of the total volume of amorphous zones in the material. This process accelerates sharply with increasing substrate temperature. Amorphous Si recrystallizes at ~550°C in a furnace,[23] while only a small temperature rise (~100°C) is needed for recrystallization during implantation.

b. P Tails: Channeling and Interstitial Diffusion

The deep tails in the P distributions from the unannealed samples (Fig. 6) have been shown to be due to channeling of a small fraction of the P atoms during the implantation.[3] Most of the channeling probably occurs at the beginning of the implantation cycle before the surface region becomes amorphous or heavily damaged. In all cases studied so far in the dose range of 10^{15}-$1.7\times10^{16}cm^{-2}$ for nominal RT implantation, the tails (beyond 2Rp) observed had P distributions in agreement with channeling effects. The P profiles in the depth range

of 2Rp-4Rp from various samples are shown in Fig. 6. It seems from Fig. 6 that at elevated temperature (>100°C implantation), the number of P atoms increased in the deeper regions of the sample. This is believed to be due to a combination of channeling and interstitial diffusion. The P atoms that were steered into the open channels subsequently penetrate even deeper via interstitial diffusion. Under these circumstances, the channeling becomes indistinguishable from interstitial diffusion.

c. Annealed Samples: Incubation Period and Nucleation of Microtwins

The annealing of a continuous amorphous layer in (111) Si is known to produce microtwins.[11,16-18] However, as can be seen from the cross-section micrographs of Figs. 1b and 2b the depth at which the microtwins nucleate becomes shallower with increasing dose. For example, in the $10^{15}cm^{-2}$ sample, the twins nucleated at a depth of 1400Å while in the $10^{16}cm^{-2}$ sample, the twins nucleated at a depth of ~900Å from the surface. No twinning occurred in the samples where severe heating occurred during the implantation (Fig. 5a). This is believed to be related to the amorphicity and stresses at the a/c interface. For the twins to nucleate a flat or faceted (111) a/c interface is essential. In the present case, although the initial specimen surface was (111), the parts of the damaged layer that were only partially amorphous recrystallized by the growth of small crystalline zones in all directions. The a/c interface became continuous and faceted with 111 only when the regrowth front reached 100% amorphous material. From this model, the wider the zone of partially amorphous material, the wider will be the zone that regrows without formation of microtwins, thus accounting for the incubation

period. This is consistent with all the observations on heated and unheated (during implantation) samples.

The SIMS profiles from the annealed samples (Figs. 1c, 2c, 3c and 5b) show the presence of two distinct components of P redistribution, the first one that starts at the surface and extends to a depth close to the original a/c interface and the second one extend beyond the interface. The former component shows no significant redistribution and the P atoms appear to be pinned after annealing while the latter component shows a remarkable redistribution on annealing at or below 850°C. These results can be explained by assuming that during the epitaxial regrowth of a Si, every atom (P or Si) in the amorphous material is placed on a substitutional site. The movement of the P atoms in the recrystallized region will subsequently occur by the diffusion mechanism normally operative at that temperature. Since at annealing temperatures $\leq$850°C, no significant diffusion is expected, the P atoms in the recrytallized region appear to be pinned. This hypothesis is further substantiated by the results of Blood[4] who implanted P into already amorphicized Si. The P distribution in this case was gaussian and there was no extended tail in the unannealed sample. Subsequent annealing of this sample showed no redistribution. Some redistribution of P on subsequent annealing at low temperatures ($\leq$850°) within the epitaxially regrown volume, such as that occurred in Figs. 1, 2, 3, and 5 may be explained by pipe diffusion since the regrown material contains a high density of dislocation lines.

For the samples that suffered substantial heating during implantation (Figs. 2 and 5), the correspondence between the width of

the a region and the pinned P region may not be obvious. This is because of recrystallization by dynamic annealing as explained above. The width of the pinned region in this case indicates the depth to which the a layer extended at a certain stage during the implantation which may be deeper than the a/c interface seen after dynamic annealing has occurred and implantation is completed. For example, in Fig. 5 the width of the pinned P region is ~2200Å which agrees well with the width of the continuous a layer that did form during the implantation before the heating occurred (Fig. 4a).

On the other hand, the P atoms below the a/c interface are randomly distributed in interstitial spaces in damaged but essentially single crystal material. These atoms migrate rapidly into the material by interstitial diffusion mechanism until they eventually occupy substitutional sites. The results from the samples annealed above 750°C do not show any significant change in the distribution of the P atoms at depths $\geq$2Rp indicating that they have already occupied substitutional sites. The complete substitutionality of P atoms in the samples annealed at 837°C was confirmed by the carrier concentration measurements included in Figs. 2c and 5b where the carrier concentration profile follows the atomic profiles exactly both near the surface as well as in the deeper regions.[24] However, for the sample annealed

at 750°C, the carrier concentration profile follows the atomic profile only over the depth range 0-Rp (Fig. 1c). The electrical activity falls sharply in the deeper regions (>Rp) indicating that a large fraction of the P atoms is still in interstitial spaces. When the same sample is heated to 950°C, the carrier concentration profile follows the atomic profiles even in the deeper regions (Fig. 7b). The nature and distribution of structural defects in this sample remained the same (Fig. 7a) as in the 750°C case (Fig. 1b). These results support the recrystallization and interstitial diffusion model proposed above.

It appears from the existing data on B, As and our data on P implanted Si that the interstitial diffusion component may be related to the mass and atomic radius of the ion. Further work on the origin of channeling of various ions during random implantation is now underway.

CONCLUSIONS

1. Continuous a layers were formed by P implantation in the dose range $1x10^{15}$-$2x10^{16}cm^{-2}$. However, the width of the a layer and sharpness of the a/c interface were sensitively dependent on the substrate temperature.
2. During recrystallization microtwins were nucleated within only a part of the apparently amorphous layer suggesting that the deeper region was not 100 amorphous.

3. All the atoms (Si and P) in the amorphous layer were placed on substitutional sites during the migration of the a/c front on subsequent-annealing and were therefore electrically active.
4. In the deeper regions (below the a/c interface), the P atoms initially diffuse rapidly into the bulk via interstitial diffusion. At high temperatures (>750°C), the P atoms are found to occupy substitutional sites.

ACKNOWLEDGMENTS

One of the authors (DKS) would like to thank his colleagues T. Sands and R. Caron for useful discussions and editing the manuscript. This work was supported by the Director, Office of Energy Research, Office of Basic Energy Sciences, Materials Research Division of the U.S. Department of Energy under Contract No. DE-AC03-76SF00098.

REFERENCES

1. D. K. Sadana, J. Washburn and G. R. Booker, Phil. Mag. (in press).

2. D. K. Sadana, M. Strathman, J. Washburn, C. W. Magee, M. Maenpaa and G. R. Booker, App. Phys. Lett. 37 615 (1980).

3. W. K. Hofker, Phil. Res. Repts. Suppl. 8 (1975).

4. P. Blood, G. Dearnaley and M. A. Wilkins, Rad. Eff. 21 245 (1974).

5. G. Dearnaley, J. M. Freeman, G. A. Gard and M. A. Wilkins, Can. J. App. Phy. 46 587 (1968).

6. R. G. Wilson, NBS Rept. No. GCR-87-325, "Measurement Technology for Critical Ion Implantation Parameters" (Dec. 1981).

7. J. M. Shannon, R. A. Ford and G. A. Gard, Rad. Eff. 6 217 (1970).

8. R. B. Fair and G. R. Weber, J. App. Phys. 44, 273 (1973).

9. D. K. Sadana, J. Washburn, M. Strathman, M. C. Current and M. Maenpaa, Inst. of Phys. Cenf. Ser. (London) 60 453 (1981).

10. R. O. Schwenker, E. S. Pan and R. F. Lever, J. App. Phys. 42 3195 (1971).

11. R. Drosd and J. Washburn, J. App. Phys. 53 397 (1982).

12. M. G. Garimaldi, B. M. Paine, M. A. Nicolet and D. K. Sadana, J. App. Phys. 52 4038 (1981).

13. J. F. Gibbons, W. S. Johnson and S. W. Mylroie, Projected Range Statistics, 2nd ed., Hutchinson and Ross (1975).

14. J. Fletcher, J. M. Titchmarsh and G. R. Booker, Ins. Phys. Conf. Ser. (London) 52 153 (1980).

15. C. W. Magee, J. Electrochem. Soc. 126 660 (1979).

16. M. D. Rechtin, P. P. Pronko, G. Foti, L. Csepregi , E. F. Kennedy, and J. W. Mayer, Phil. Mag. 37, 605 (1978).

17. G. Foti, L. Csepregi, E. F. Kennedy, J. W. Mayer, P. P. Pronko and M. D. Rechtin, Phil. Mag. 37, 591-604.

18. L. Csepregi, J. W. Mayer and T. W. Sigmon, App. Phys. Lett. 29, 92 (1976).

19. B. J. Masters and J. M. Fairfield, Rad. Eff. 6 57 (1970).

20. P. F. Byrne, N. W. Cheung and D. K. Sadana, App. Phys. Lett. 41, 537 (1982).

21. J. Washburn, C. S. Murty, D. K. Sadana, P. Byrne, R. Gronsky, N. W. Cheung and R. Kilaas, Intern. Conf. on Ion Beam Modification of Materials, Grenoble (France) September 6-10, 1982.

22. D. K. Sadana, J. Washburn, P. F. Byrne and N. W. Cheung, Defects in Semiconductors, Materials Research Society, Boston Nov. 1-4 (1982) (to be published).

23. J. W. Mayer, L. Csepregi, J. Gyulai, T. Nagy, G. Mezey, P. Revesz and E. Kotai, Thin Solid Films 32, 303 (1976).

24. The maximum carrier concentration that can be measured reliably by the spreading resistance technique is $\sim 2\times10^{20}cm^{-3}$. (D. Dickey, Solecon Labs, Sunnyvale, CA, private communication.) Therefore, apparent lower electrical activity near the peaks in Figs. 2c and 5b should not be taken to represent complex or precipitation formation at P concentrations $\geq 2\times10^{20}cm^{-3}$.

FIGURE CAPTIONS

Fig. 1. $P^+ \rightarrow$ (111) Si, $10^{15}cm^{-2}$, 120 keV, room temperature implantation (a) XTEM micrograph from unannealed specimen shows a continuous amorphous layer, (b) XTEM micrograph from 750°C annealed specimen shows microtwins (L) and a layer of dislocations loops (M) (c) P profiles from specimens (a) and (b), and carrier concentration profile from specimen (b).

Fig. 2. $P^+ \rightarrow$ (111) Si, $10^{16}cm^{-2}$, 120 keV, implantation temperature ~100°C (a) XTEM micrograph from unannealed specimen (b) XTEM micrograph from 837°C annealed specimen (c) P profiles from specimens (a) and (b), and carrier concentration profile from specimen (b).

Fig. 3. $P^+ \rightarrow$ (111) Si, $1.7 \times 10^{16}cm^{-2}$, 120 keV, room temperature implantation (a) XTEM micrograph from unannealed specimen (b) P profiles from specimen (a) before and after annealing at 837°C.

Fig. 4. $P^+ \rightarrow$ (111) Si, $7.5 \times 10^{15}cm^{-2}$, 120 keV, implantation temperature ~350°C (varied across the wafer), XTEM micrographs (a) through (d) showing single and multiple amorphous layers and (e) a buried layer of small dislocation loops.

Fig. 5. (a) An XTEM micrograph from the specimen obtained after annealing at 850°C of one of the defect structures shown in Fig. 6, (b) P profiles before and after the annealing of the specimen of Fig. 7a, and carrier concentration profile from the annealed specimen.

Fig. 6. Phosphorus tail distributions in the depth range 2Rp–4Rp from all the unannealed specimens used in this study.

Fig. 7. Inplantation conditions same as in Fig. 1. (a) XTEM micrograph from the 950°C annealed specimen. The dense band extending from the surface contains microtwins, dislocations, etc. (b) P and carrier concentration profiles corresponding to the specimen of (a).

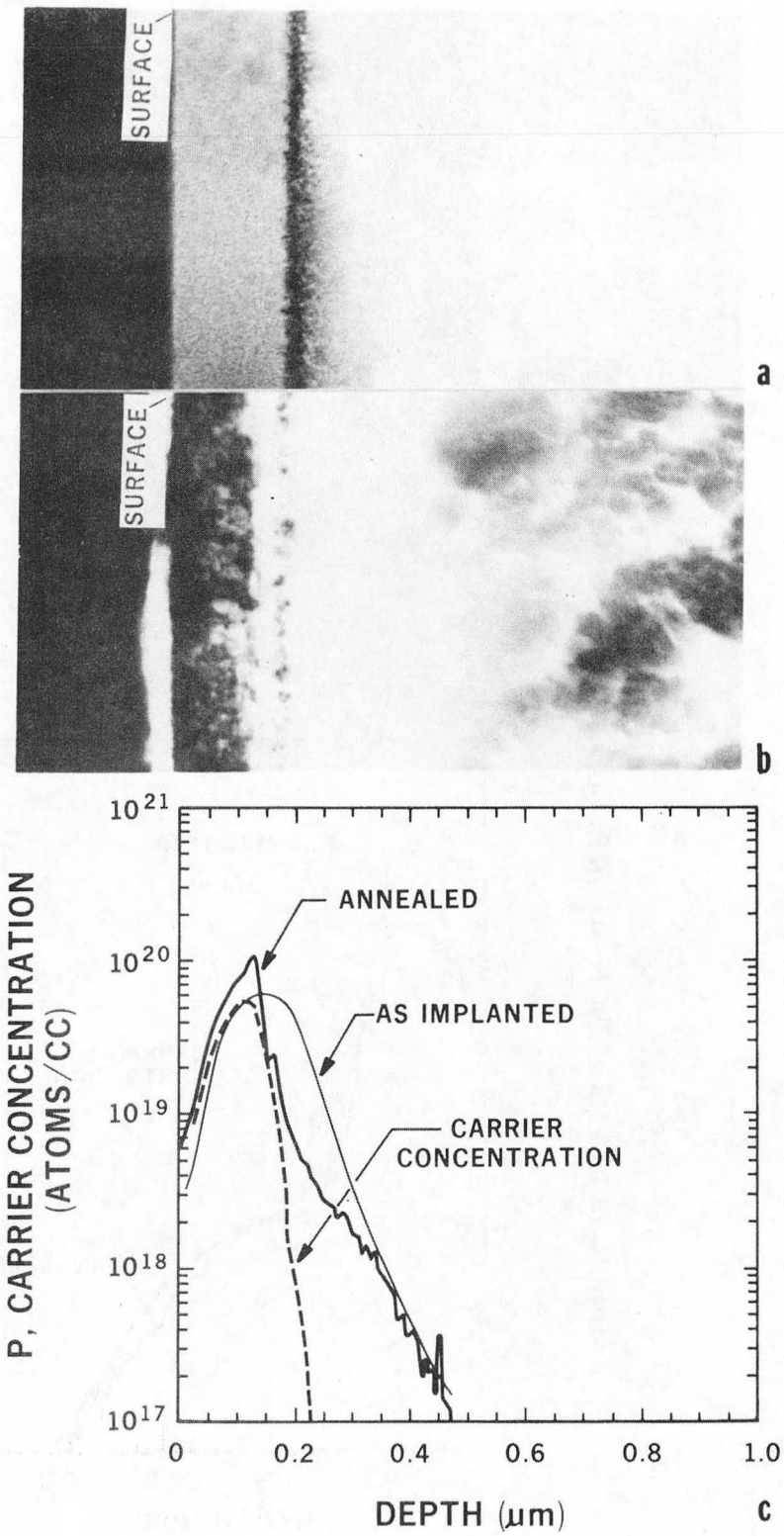

Fig. 1 XBB 828-6859

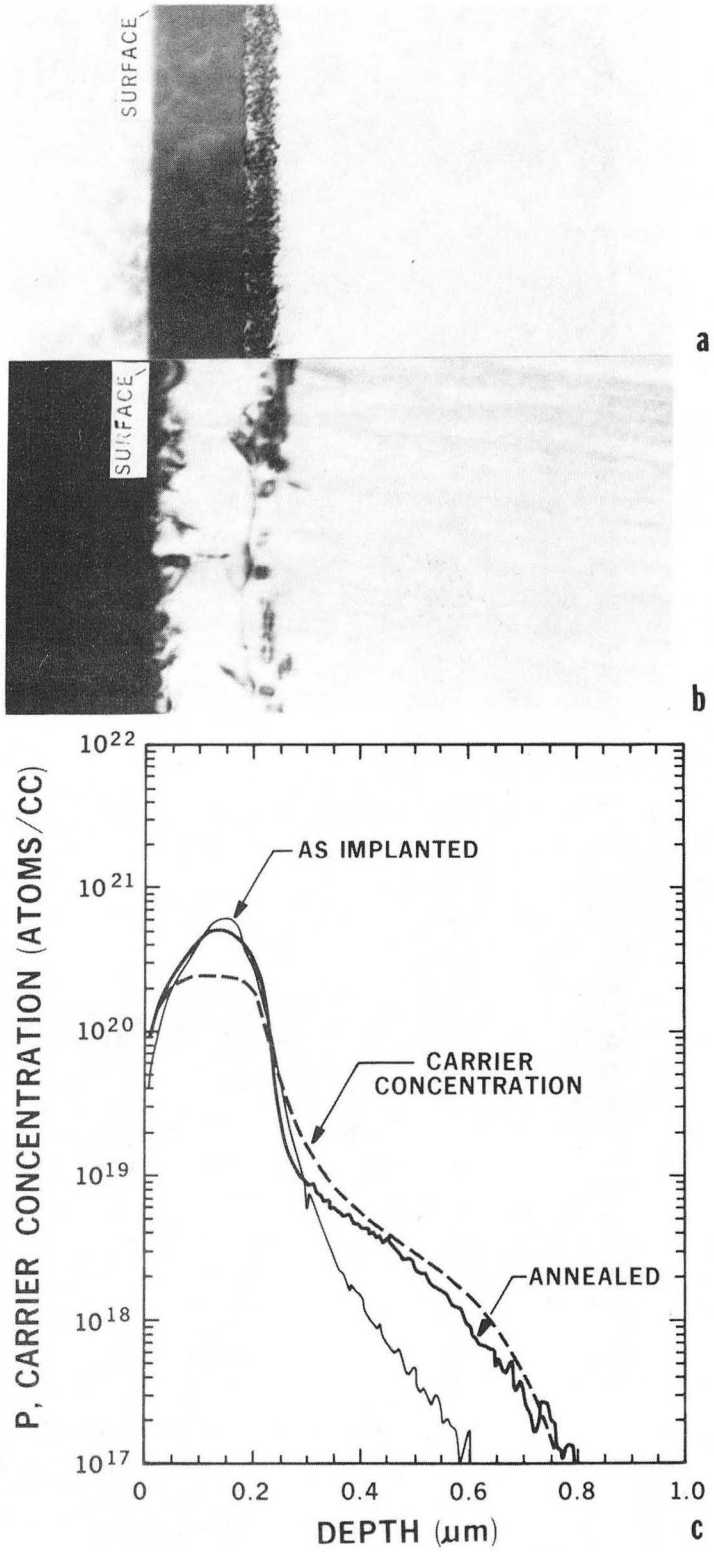

Fig. 2 XBB 828-6858

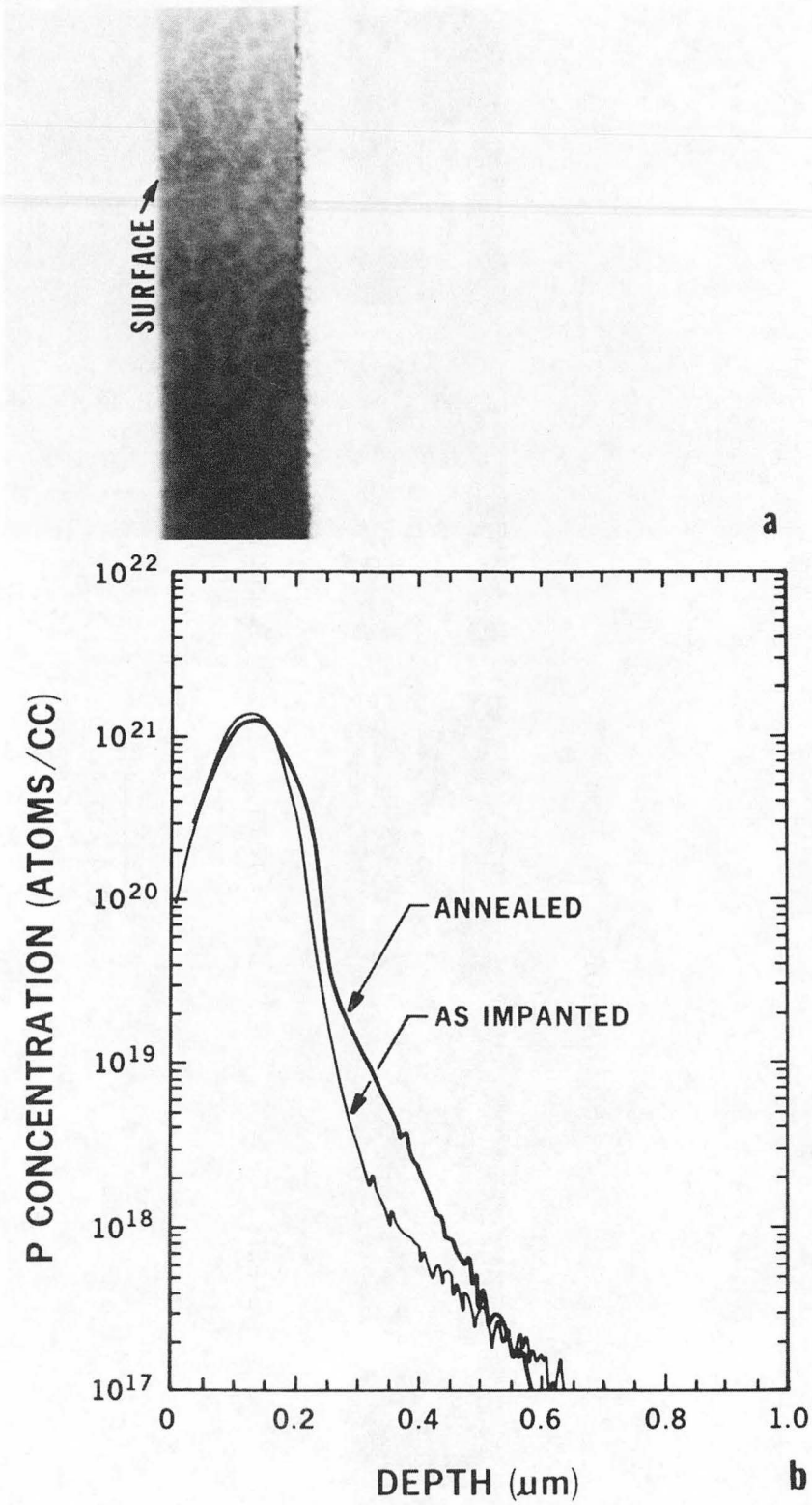

Fig. 3 XBB 828-6857

Fig. 4 XBB 790-15689

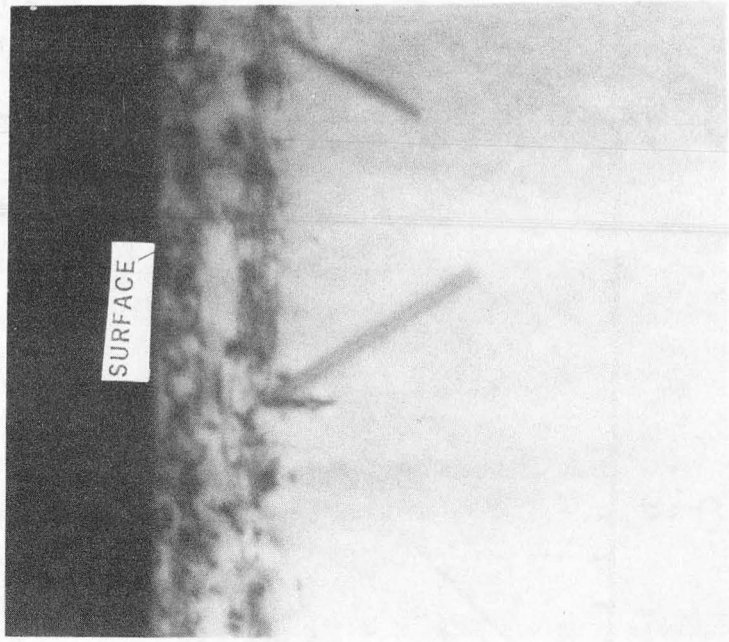

a

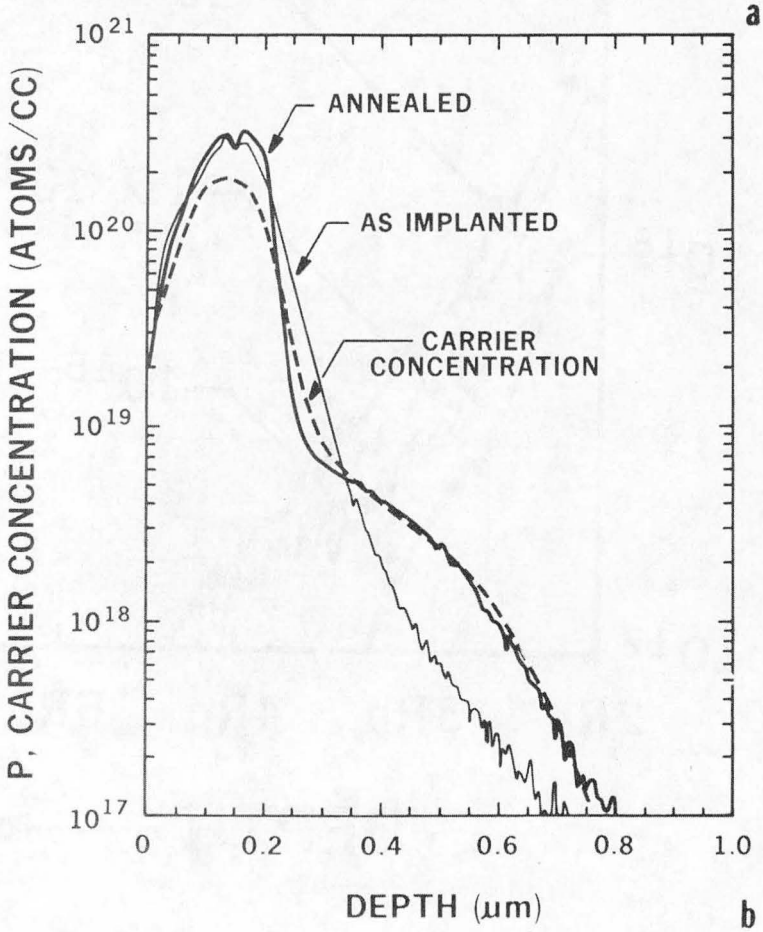

b

Fig. 5 XBB 828-6855

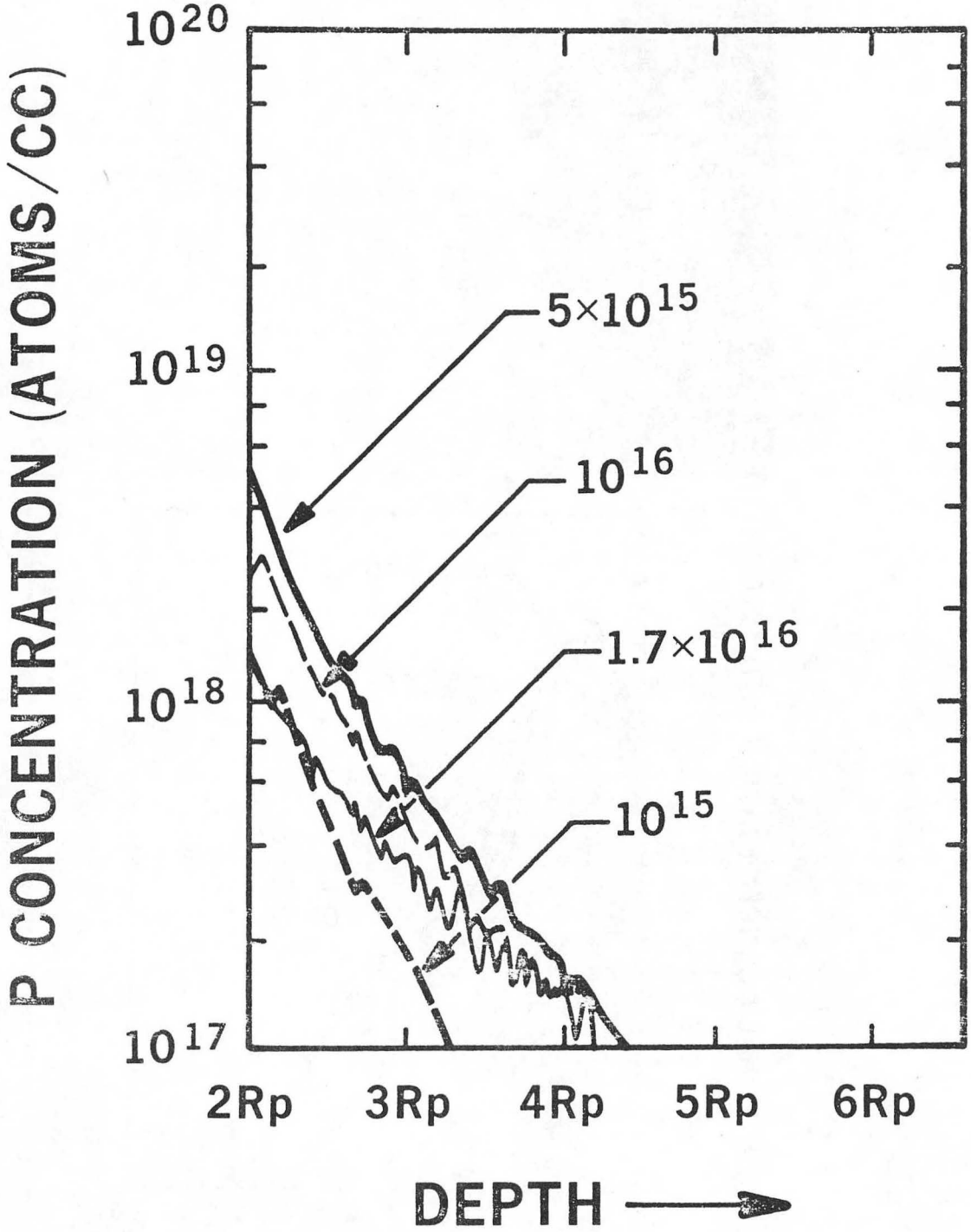

Fig. 6

XBL 828-11003

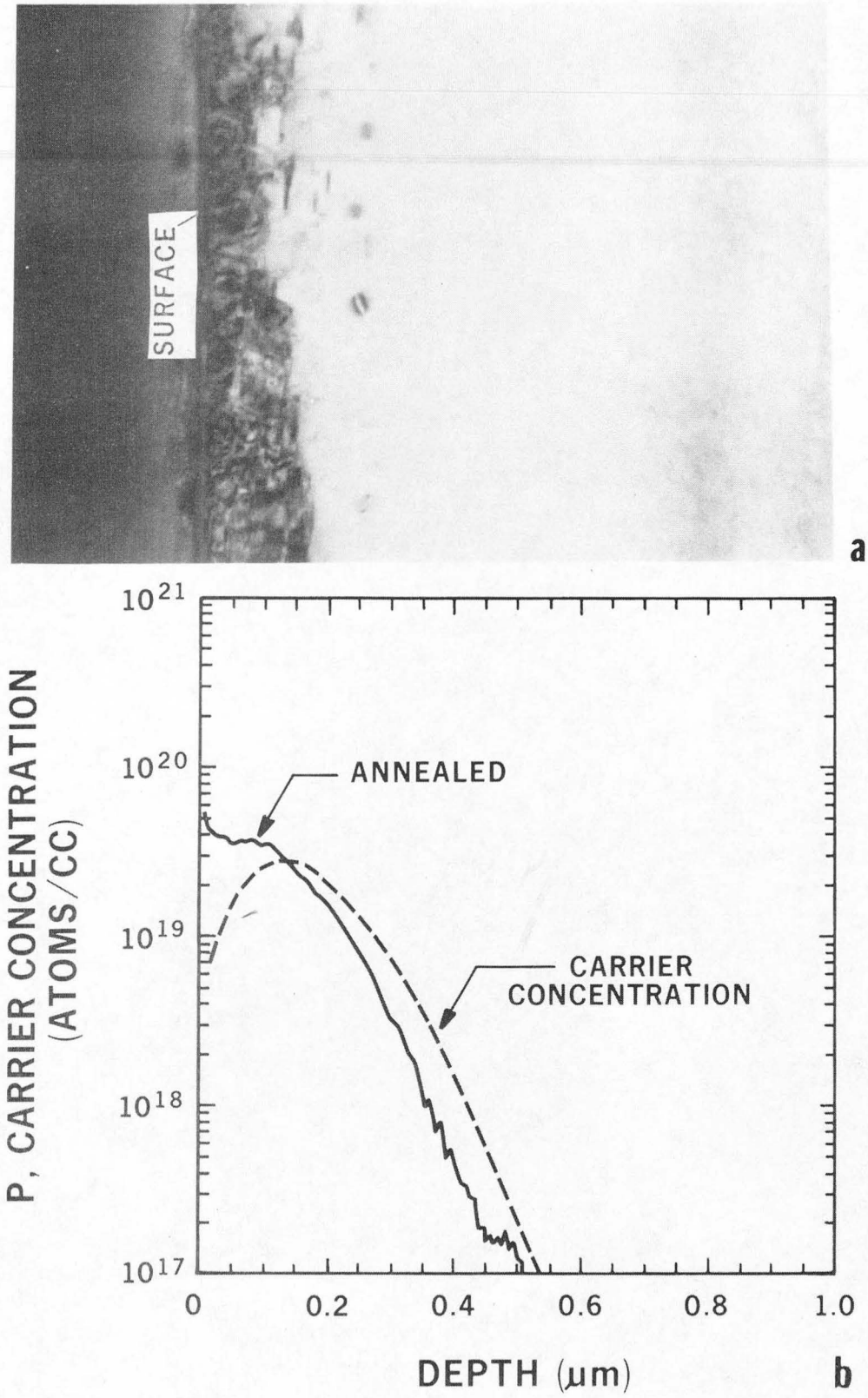

Fig. 7 XBB 828-6861

This report was done with support from the Department of Energy. Any conclusions or opinions expressed in this report represent solely those of the author(s) and not necessarily those of The Regents of the University of California, the Lawrence Berkeley Laboratory or the Department of Energy.

Reference to a company or product name does not imply approval or recommendation of the product by the University of California or the U.S. Department of Energy to the exclusion of others that may be suitable.

TECHNICAL INFORMATION DEPARTMENT
LAWRENCE BERKELEY LABORATORY
UNIVERSITY OF CALIFORNIA
BERKELEY, CALIFORNIA 94720